

## Article

# Numerical Investigation on Deep-Foundation Pit Excavation Supported by Box-Type Retaining Walls

Peng Peng <sup>1</sup>, Weiyao Kong <sup>1</sup>, Saishuai Huang <sup>1</sup>, Yi Long <sup>2</sup> and Yang Lu <sup>2,\*</sup> <sup>1</sup> Shanghai Municipal Engineering Design Institute (Group) Co., Ltd., Shanghai 200092, China<sup>2</sup> College of Water Conservancy and Hydropower Engineering, Hohai University, Nanjing 210098, China

\* Correspondence: luy@hhu.edu.cn

**Abstract:** In soft soil foundations, the utilization of box-type retaining walls as a support method represents a novel approach. This study focuses on investigating the key factors influencing lateral wall deflection and ground settlement behind the wall in deep excavation projects supported by box-type retaining walls. Based on a practical engineering case in Shanghai, the large deformation Lagrangian numerical simulation software FLAC-3D is employed to simulate the displacement of box-type retaining walls as well as the surface settlement surrounding the excavation pit during the excavation process of deep-foundation pits. This research encompasses aspects such as the box size, the filling material within the box, and the constituent materials of the retaining wall. Ultimately, it is concluded that variations in the size of the box-retaining wall have a significant impact on wall deflection and surrounding ground settlement, while the filling material and constituent materials have relatively minor effects. This study provides a theoretical basis and scientific reference for the design and construction of box-type retaining walls in deep-foundation pit engineering.

**Keywords:** foundation pit; box-type retaining wall; lateral deflection; surface settlement; numerical simulation



Academic Editor: Eugeniusz Koda

Received: 29 September 2024

Revised: 25 November 2024

Accepted: 29 November 2024

Published: 31 December 2024

**Citation:** Peng, P.; Kong, W.; Huang, S.; Long, Y.; Lu, Y. Numerical Investigation on Deep-Foundation Pit Excavation Supported by Box-Type Retaining Walls. *Buildings* **2025**, *15*, 109. <https://doi.org/10.3390/buildings15010109>

**Copyright:** © 2024 by the authors. Licensee MDPI, Basel, Switzerland. This article is an open access article distributed under the terms and conditions of the Creative Commons Attribution (CC BY) license (<https://creativecommons.org/licenses/by/4.0/>).

## 1. Introduction

In recent years, China's urbanization has accelerated, leading to larger cities, increased sewage, and scarce land for planning. Urban sewage treatment plants are shifting toward integration and underground development, resulting in larger water-treatment structures, deeper foundation pits, and complex environments. Limited land and construction time necessitate innovative approaches for deep-foundation pit engineering [1]. For deep-foundation pit projects with large excavation depths and strict displacement control, the self-standing retaining system represented by cantilever structures is a commonly used support method, such as double-row piles and cellular diaphragm walls. It features high overall rigidity and does not require a support system, allowing it to withstand significant water and soil pressures [2,3]. Moreover, the retaining walls, as a kind of effective support structure, are widely used in highway, railway, water conservancy, and hydropower projects but rarely in municipal foundation pit projects, especially in foundation pit projects with complex surrounding environments, soft foundation soil, large foundation pit areas, and deep depths [4–6]. There are various types of retaining walls, and the common structural types in practical engineering include gravity retaining walls, counterfort retaining walls, cantilever retaining walls, buttressed retaining walls, etc. [7]. Through these supported structures of deep excavation systems, the deflection behavior, commonly involving lateral wall deflection, and ground settlement behind the wall are well controlled [8–10].

With the development of the retaining wall used in deep-foundation pits, many new retaining structures have emerged, one of which is the box-type retaining wall structure [11]. Box-type retaining walls and similar structures (such as lattice retaining walls), as a form of underground retaining structure, have developed rapidly in recent years [12,13]. Filled with plain soil, stone, and other materials and enclosed by reinforced concrete structures on the outside, they can save a large amount of concrete materials and reduce manufacturing costs [14]. It is also a retaining structure used to support and reinforce the fill or hillside soil to prevent its collapse and maintain stability [15,16]. Its basic structural type is similar to the empty box we see in our daily life, which is closed on all sides with an empty interior. Due to its unique geometric structure, the box-type retaining wall structure has greater overall rigidity and good stability, which can better control the deformation of the foundation pit. Moreover, it does not need to set up an internal support system, and it can be used as a permanent retaining structure. Previous usage of such box-type retaining walls for conventional slope support has proven to be effective under optimized design, particularly in poor geological conditions, where improved designs can significantly reduce construction costs and enhance structural stability and safety [17]. As a new retaining structure in the usage of deep-foundation pit engineering, the box-type retaining wall structure method has been applied for a relatively short time, and because of its complex form, the progress of its theoretical and numerical research is far behind the development of engineering practice.

To analyze the factors influencing the supporting effect of box-type retaining walls in soft soil foundations in Shanghai, this paper utilizes Hypermesh software (version 2019) to establish a three-dimensional model of the foundation pit. The FLAC-3D software is then employed to calculate the actual working conditions, and the obtained results are compared with actual monitoring data to indirectly verify the reliability of the simulation results. Based on this, the deflection behavior of deep excavation systems, including lateral wall deflection and ground settlement behind the wall, are analyzed and discussed. Also, three different influencing factors, namely, the size of the box-type retaining wall, the filling material within the box, and the constituent materials, are varied, and corresponding results are calculated separately. Furthermore, the influence pattern of each factor is analyzed. The research findings are expected to provide a certain scientific reference for the design and application of box-type retaining walls in soft soil areas.

## 2. Project Information

### 2.1. General Description of Foundation Pit

A project of sludge treatment and disposal of Bailonggang Wastewater Treatment Plant is located in the open space on both sides of the existing anaerobic digestion tanks of Bailonggang Wastewater Treatment Plant, with Plot 01 located on the northeast side of the anaerobic digestion tanks (Figure 1a). The project is located in a soft soil area of a coastal city, where weak intercalated layers exist within the soil strata. Given the land constraint during construction, the adoption of box-type retaining walls enables unsupported excavation, thereby reducing the occupation of construction land. The project mainly includes a mud storage pond, a sludge dewatering workshop, a sludge drying and incineration workshop, a rainwater and sewage pump house, and several deodorization equipment foundations, all of which are arranged in the sunken plant area.

The sunken plant area of Plot 01 has a plan size of  $179.2\text{ m} \times 169.8\text{ m}$ , with burial depths of 13.6 m ( $9875.7\text{ m}^2$ ), 10.6 m ( $5296.3\text{ m}^2$ ), and 6.8 m ( $11,048.7\text{ m}^2$ ), respectively, covering a total area of  $26,220.7\text{ m}^2$  (Figure 1b). Due to the requirements of equipment and the surrounding environment, it is impossible to set up upper supports or floor slabs under permanent working conditions, resulting in a sunken plant structure. Therefore,

an ultra-deep box-type retaining wall structure can be designed in combination with the deep-foundation pit enclosure system of the sunken plant area to meet the operational management requirements under the permanent working conditions of this project.

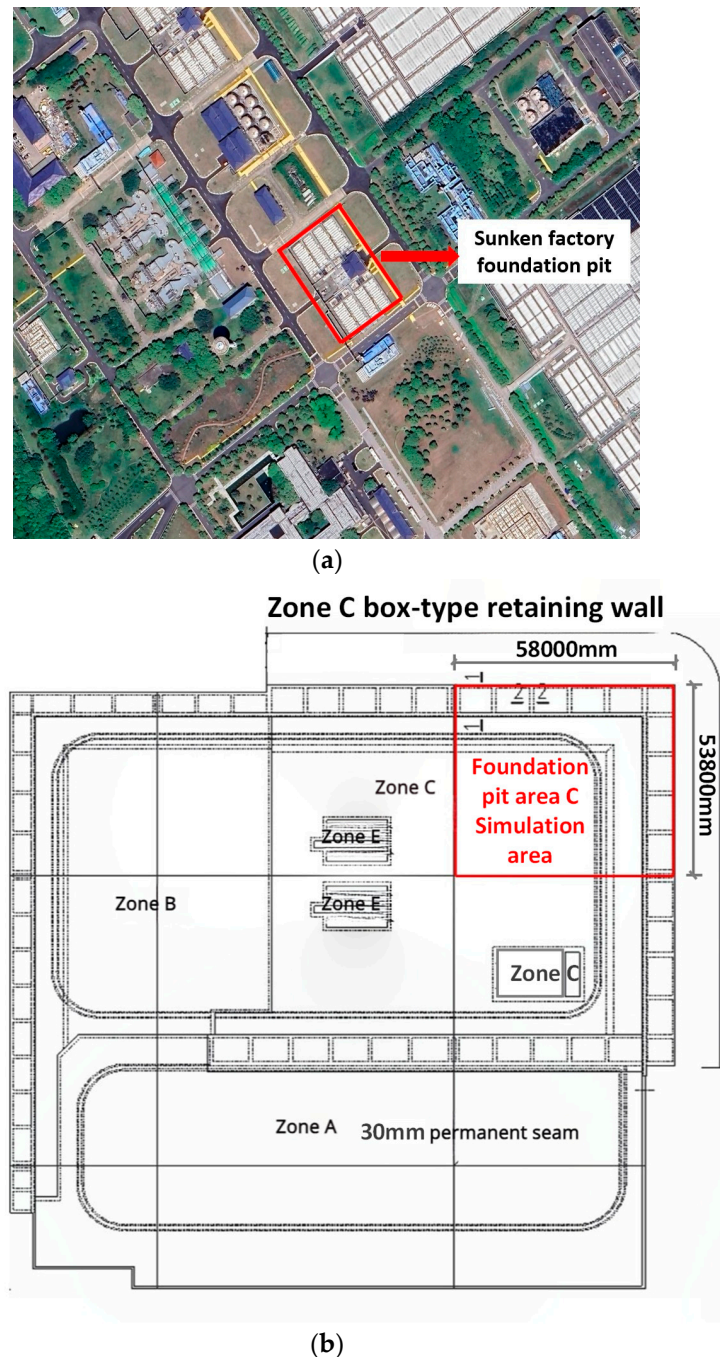


**Figure 1.** Location of the considered project: (a) picture of foundation pit zoning; (b) graphic layout of foundation pit zoning.

Figure 2 shows some typical pictures of the construction process of the foundation pit. During the construction of the foundation pit, the soil body at the box-type retaining wall was first excavated, and the supporting was properly performed, and then, the box-type retaining wall was poured layer by layer, as shown in Figure 2a. After the box-type cantilever retaining wall structure met the design strength of 30 MPa (C30), the remaining earthwork inside the retaining wall was excavated to the bottom of the pit, as shown in Figure 2b. Finally, the construction of the box-type retaining wall structure and foundation

pit excavation was completed, as shown in Figures 2c and 2d, respectively. Figure 2e shows the schematic diagram for lateral deformation (inclinometry) monitoring of retaining walls. The wall deformation is assessed using the Newgeometrics Inclinometer from the USA, comprising the Digitilt Data Mate II readout device, Digitilt Inclinometer series probe, and cable transmission line. The system features a total measurement range of  $\pm 53^\circ$ , precision of  $\pm 0.01$  mm/500 mm, and sensitivity of  $\pm 10$  arc-seconds ( $\pm 0.05$  mm/m). The recorded data are employed to generate lateral deformation curves of the retaining wall.

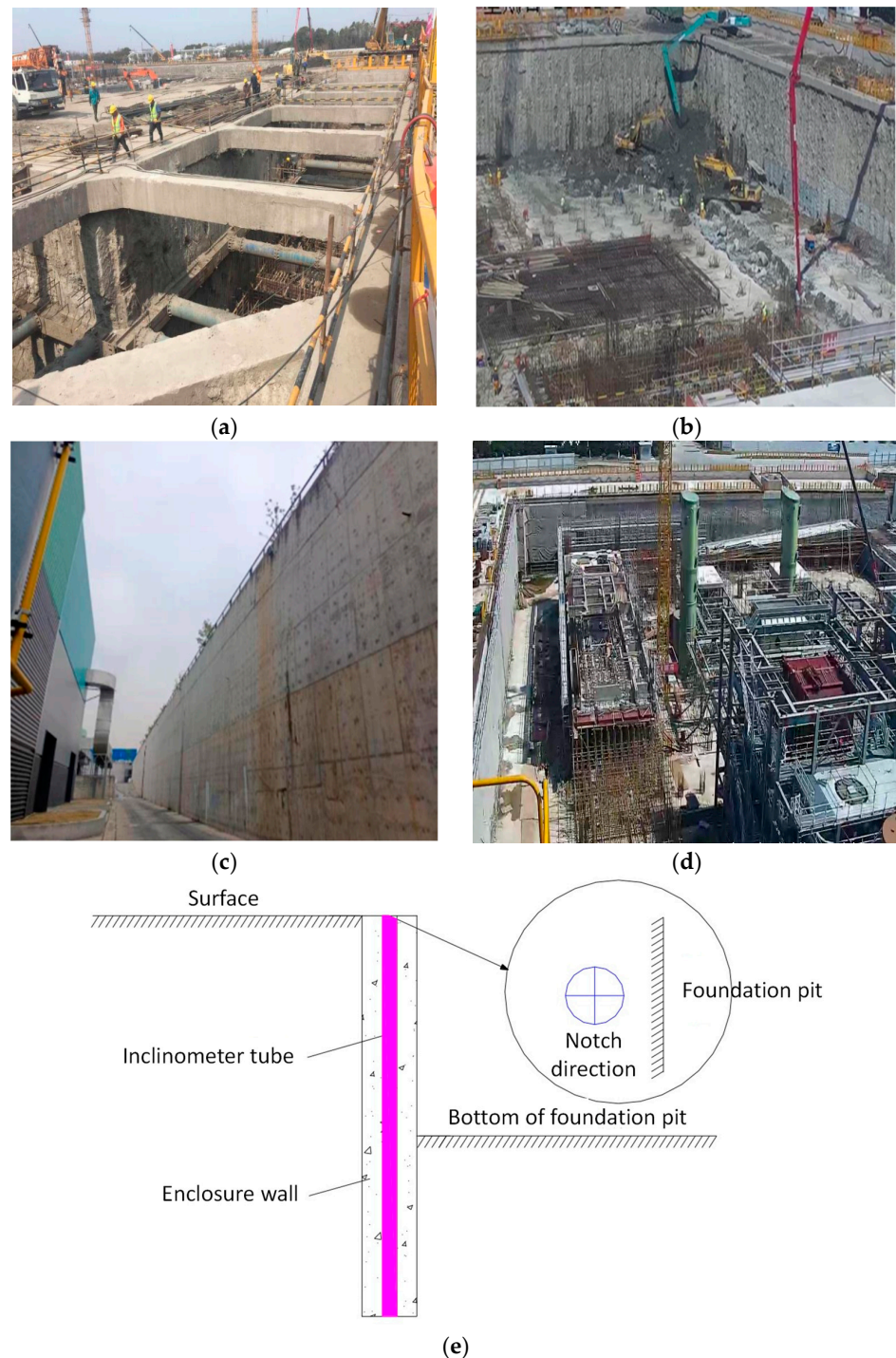


**Figure 2.** Construction site images: (a) Excavation of pit inside box-type retaining wall; (b) Excavation construction of the foundation pit to the bottom; (c) Completed box-type retaining wall; (d) Completed foundation pit site; (e) Schematic diagram for lateral deformation (inclinometry) monitoring of retaining walls.

## 2.2. Overview of Foundation Pit Support and Geological Conditions

Figure 3a shows the typical location profile before the excavation of the foundation pit, a cross-section of the foundation pit with the novel box-type retaining wall. The site is leveled to  $-1.40$  m. A slope ratio of 1:1.5 is adopted, and then, the enclosure structures are constructed, mainly including bored piles, triaxial mixed piles, and diaphragm walls. In addition, rotary jet grouting reinforcement is performed at the weak soil layer, which plays a role in restricting the horizontal and vertical displacements of the passive zone within the pit.

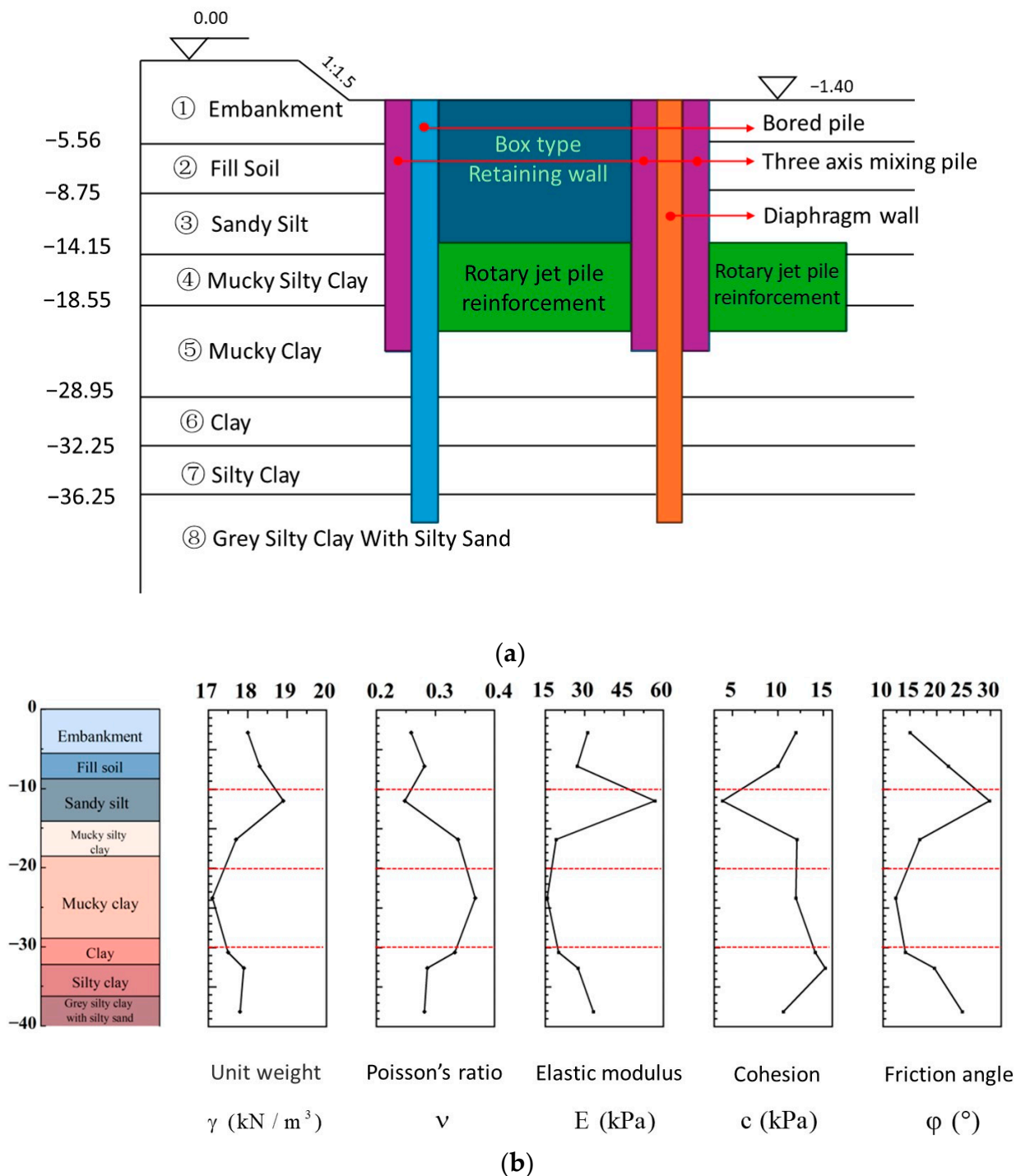


**Figure 3.** (a) The cross-section of the foundation pit with box-type retaining wall. (b) Soil profiles and material properties at the site.

Prior to the commencement of construction, a rigorous exploration of the subsurface conditions and soil properties at the site was undertaken through a comprehensive suite of in situ and laboratory tests, such as specific gravity testing, consolidation testing, compression testing, etc. [18]. Figure 3b provides a condensed representation of the soil profiles, encompassing the depth-wise variation in soil layers, along with a selection of measured soil properties. The soil characteristics depicted in this figure are predominantly derived from the meticulous analysis of test results, ensuring their accuracy and reliability. The stratigraphy presented is a representative average derived from extensive data collection across the site, thereby providing a holistic understanding of the subsurface geology. According to the on-site exploration data, within the exploration depth range, the foundation soil distribution is relatively stable, and the soil layers can be divided into six major layers and several sub-layers from top to bottom. Among them, layer ① is mainly composed of hydraulic fill (silty soil mixed with cohesive soil), and the upper part of some sections is miscellaneous fill; layers ② to ⑧ are Holocene Q4 sedimentary layers.

### 3. Three-Dimensional Numerical Simulation

Based on the aforementioned project status, this chapter utilizes FLAC 3D software and adopts the large deformation Lagrangian numerical simulation method [19] to conduct three-dimensional numerical simulation calculations of the excavation process of the foundation pit at the Wastewater Treatment Plant project. This is performed to simulate the stress release of the excavation soil and the resulting deformation of the surrounding environment of the foundation pit [20,21]. This analysis mainly focuses on the deformation of the foundation pit support structures, as well as the impact of the excavation construction on the surrounding environment.

#### 3.1. Three-Dimensional Model Establishment

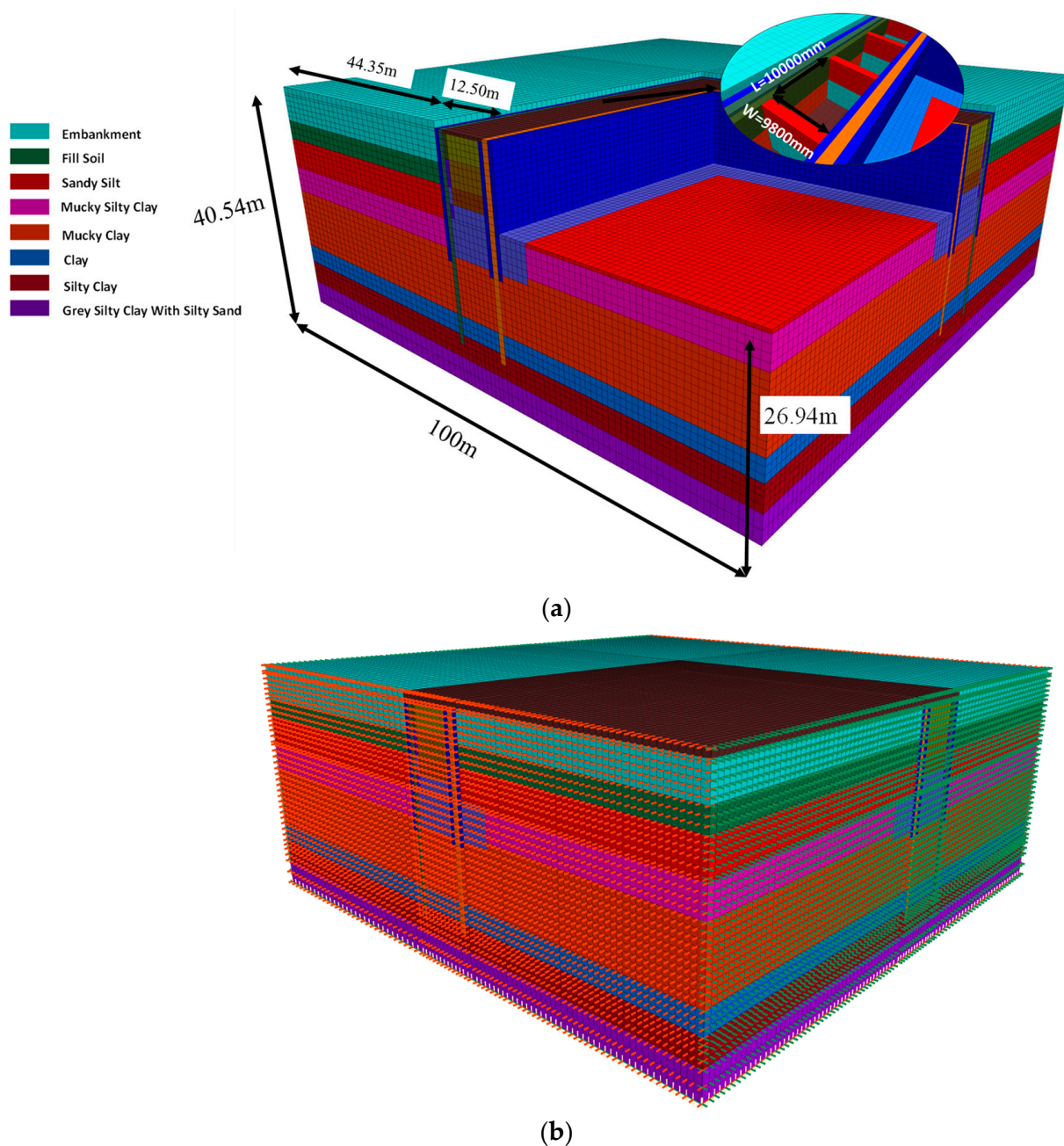
Given the boundary effect of this model and the range of spatial effects, the modeled area covers about one-fourth of the region. Also, practical engineering advice sets the soil scope around the pit at three times its depth, yielding realistic calculations. Therefore, the dimensions of this model are chosen to be 58 m long, 48 m wide, and 40.5 m deep. The length of the foundation pit in the eastern area is determined to be 80 m, while the length of the foundation pit in the western area is determined to be 72 m, with a width of 32 m and an excavation depth of 15.4 m. Horizontal constraints are imposed on the lateral sides of the model, vertical constraints on the bottom, and a free boundary on the top surface.

The box-type retaining wall primarily consists of a foundation, reinforced concrete structures, and filling materials. The concrete structures are comprised of a front wall, a rear wall, intermediate partitions, vertical partitions, a base plate, a top plate, and other components. During construction, the front wall of the box-type retaining wall serves as part of the underground diaphragm wall, with its material parameters set identical to those of the underground diaphragm wall. The other parts are made with C30 concrete, and the filling inside the box is taken from the surface filling of the foundation pit. The three-dimensional models of the foundation pit are depicted in Figure 4a.

The model was automatically grouped into six distinct faces using the grouping function of FLAC 3D. To accurately simulate the lateral deformation characteristics of the box-type retaining wall under the excavation of foundation pits, horizontal constraints were applied around the model, and vertical constraints were applied at the bottom to restrict horizontal and vertical displacements. The top was set as a free boundary, as shown in Figure 4b.

The retaining structures and supports are considered elastic materials, with their material parameters outlined in Table 1. The foundation pit is retained using an under-

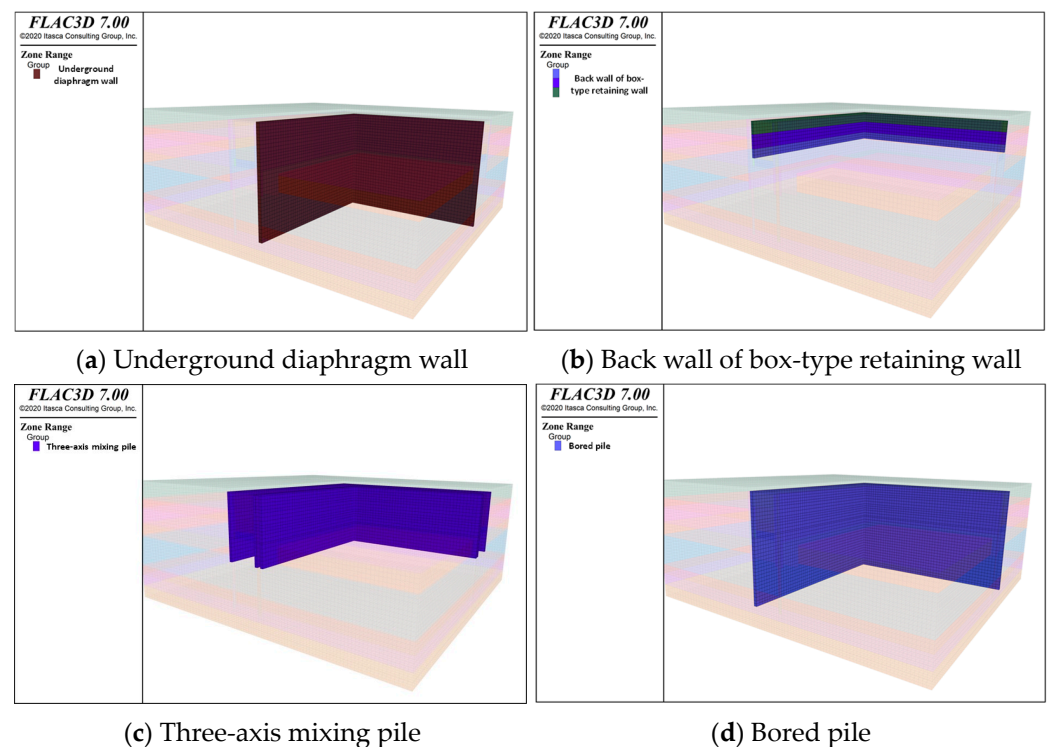
ground diaphragm wall (wall thickness: 800 mm, depth: 32.0 m, concrete grade: C30) and bored piles (pile diameter: 1000 mm, spacing: 1200 mm, pile length: 32.0 m, concrete grade: C30). The water-stopping for the bored piles employs triaxial soil mixing piles (diameter:  $\phi 850@600$ , pile length: 18.2 m). During simulation calculations, due to the continuity of bored piles and triaxial soil mixing piles, the row piles can be regarded as an underground diaphragm wall with different material parameters. The box-type retaining wall's bottom bearing piles adopt  $\phi 1000$  bored piles with a length of 25 m and concrete grade C30. The pit bottom is reinforced with a grid pattern of high-pressure jet grouting piles. During calculations, the bearing piles are simulated using structural elements, while the reinforcement area at the pit bottom enhances the physical and mechanical properties of the corresponding soil mass. The detailed numerical simulation model of various retaining structures is shown in Figure 5.



**Figure 4.** Numerical simulation model. (a) FLAC 3D calculation model of the whole foundation pit. (b) Model boundary conditions.

**Table 1.** Material parameters of the enclosure structure.

Structure Name	Unit Type	Elastic Modulus/GPa	Poisson Ratio	Unit Weight /(kN/m <sup>3</sup> )	Size
Underground continuous wall	Solid Elements	30	0.3	24.5	Thickness 800 mm
Back wall of box-type retaining wall	Solid Elements	30	0.2	17.8	Thickness 800 mm
Three-axis mixing pile	Solid Elements	30	0.2	24.5	Pile diameter 850 mm
Bored piles	Solid Elements	30	0.2	24.5	Pile diameter 1000 mm

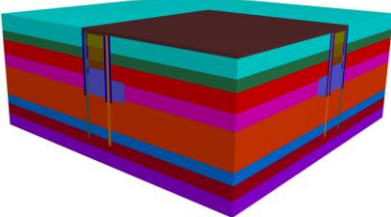
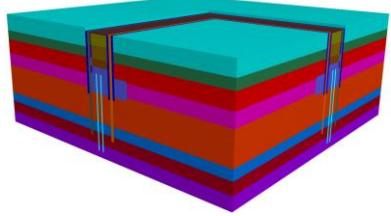
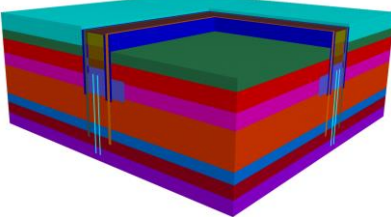
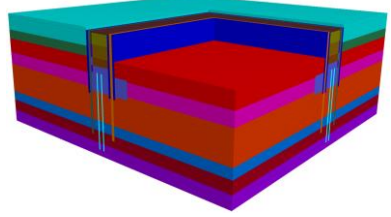
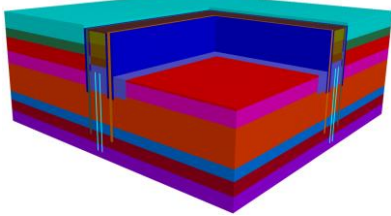
**Figure 5.** Detailed numerical simulation model. (a) Underground diaphragm wall. (b) Back wall of box-type retaining wall. (c) Three-axis mixing pile. (d) Bored pile.

The soil constitutive model utilized in this model is calculated using the Mohr–Coulomb model. The criterion excels in foundation pit excavation calculations, capturing soil’s tensile–compressive asymmetry with simple, measurable parameters, yielding reliable results widely used in geotechnical engineering [22,23]. It partially simulates hydrostatic pressure’s impact, which is vital for soil stability analysis. However, its sharp yield surface causes plastic flow inconsistencies, complicating calculations and slowing convergence. Moreover, it fails to fully capture stress–yield relationships and stress path effects, potentially leading to prediction deviations, especially significant surface rebound during initial excavation, differing from actual experience [24,25].

### 3.2. Construction Process

In the actual project, the foundation pit excavation is a layered excavation, not a one-time excavation to the bottom of the foundation pit. In order to simulate the dynamic process of the foundation pit excavation in the actual project, five processes are set up according to the actual construction sequence, as shown in Table 2.

**Table 2.** Foundation pit excavation procedure.

Step	Construction Process	Construction Diagram
Step 1	Stress balance	
Step 2	Apply envelope structure and box-type retaining wall	
Step 3	Excavation of 1st layer of soil (4.7 m); Pump to 5.7 m	
Step 4	Excavation of 2nd layer of soil (8.0 m); Precipitation to 14.6 m	
Step 5	Excavation of 3rd layer of soil (13.6 m); Precipitation to 14.6 m	

### 3.3. Model Rationality Verification

To validate the reliability of software simulation results, displacement diagrams of the front and back walls of the box-type retaining wall, derived from actual engineering monitoring data, were compared with those simulated by FLAC-3D, as illustrated in Figure 6. The figure reveals a high degree of agreement between the simulated values and monitored data within the depth range of the box-type retaining wall, approximately 0–15 m, which indirectly demonstrates the credibility of the numerical simulation. It can be observed that there are errors between field monitoring and simulations, particularly in soft soil layers, due to complex soil conditions, which can lead to deviations in simplified simulation methods [26,27]. However, this paper ensures a high degree of agreement between the measured lateral displacements within the height range of the box-type retaining wall and the simulated values. Specifically, the monitoring and simulation results at a depth of 10 m from the pit bottom remain approximately equal, and the trends of the two curves are generally the same. Therefore, the simulation results within the range of

the box-type retaining wall can be considered reliable, allowing for subsequent numerical simulation calculations based on them. Yet, the high precision of these results is limited to the height range of the box-type retaining wall.

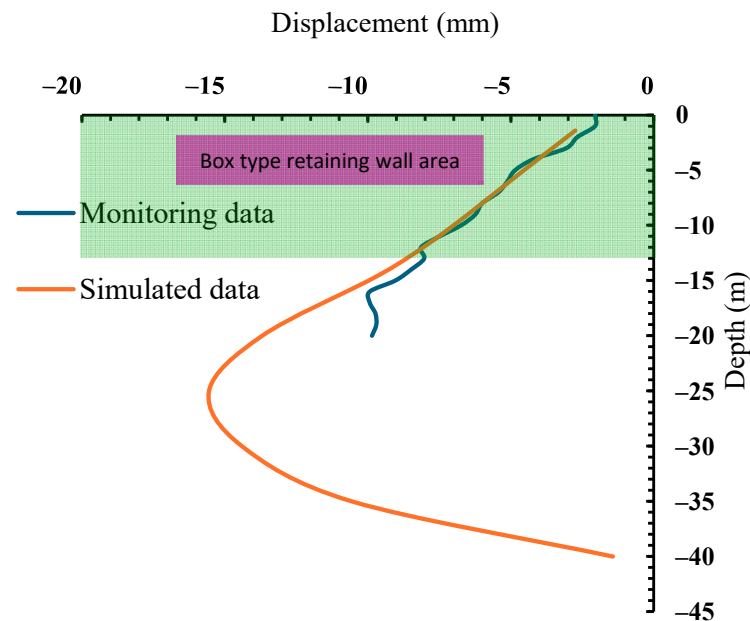


**Figure 6.** Comparison of measured and simulated deformations at measurement location of the front wall of the box-type retaining wall displacement.

## 4. Results and Discussion

### 4.1. Settlement of Foundation Pit Bottom and Surrounding Site Surface

During the excavation process of a foundation pit, each excavation phase results in a loss of self-weight stress within the soil mass. As excavations progress, significant rebound occurs in the center of the pit, while lesser rebound is observed on the pit's sides. With the continuous deepening of the excavation, the soil mass surrounding the foundation pit experiences varying degrees of settlement due to the excavation of internal soil and the presence of weak soil layers.

According to general principles of soil mechanics and geotechnical engineering, during the excavation of soil within the foundation pit, the surrounding soil tends to displace toward the interior of the pit. However, the presence of the box-type retaining wall as a supporting structure restricts the horizontal displacement of the soil. Nevertheless, the weak soil beneath the box-type retaining wall possesses a certain degree of creep, which causes it to deform and creep from the pit's periphery toward its interior, ultimately leading to soil expansion in the pit's center and settlement of the soil surrounding the pit. Due to the presence of the box-type retaining wall and bearing piles, they impose a certain degree of restraint on the weak soil layers, resulting in relatively minor settlement of the soil mass surrounding the foundation pit.

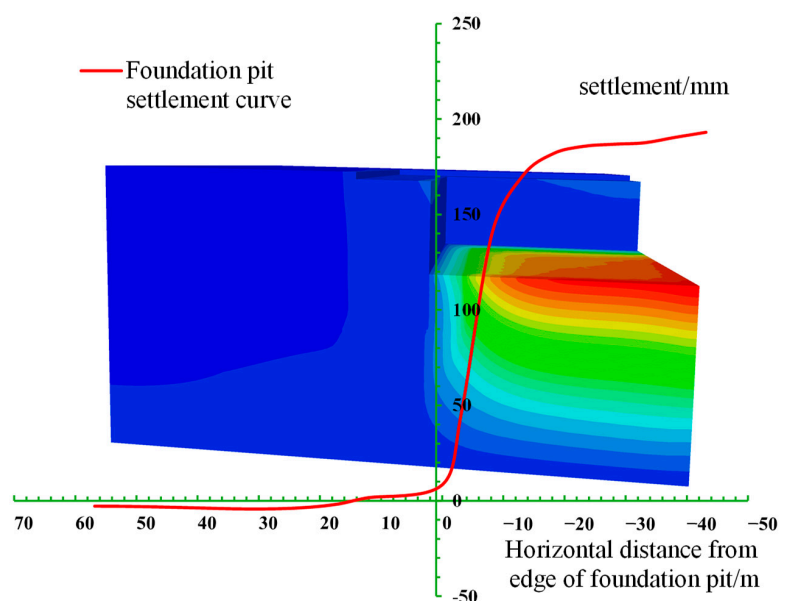
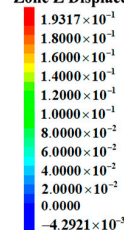
As depicted in Figure 7a, the interior and exterior of the excavation pit exhibit different patterns: the interior undergoes expansive deformation, while the surrounding ground surface outside the pit experiences settlement deformation. It is observed that significant soil expansion occurs in the center of the foundation pit, reaching 19.3 cm. Furthermore, particular attention should be given to the settlement deformation of the ground surface surrounding the exterior of the excavation pit. Calculation results indicate that the maximum surface settlement that occurred at a distance of 31.85 m from the pit is 4.25 mm, which is less than the alert threshold value of 20 mm set for monitoring surrounding surface settlements. This suggests that the settlement values of the surrounding surface are within

a controllable range. The model calculation results are consistent with the general soil settlement patterns observed during foundation pit excavation [28,29]. Figure 7b presents the envelope diagram of ground surface settlement, denoted as  $\delta_v$ , with all coordinates in the diagram being dimensionless. In this figure,  $D$  represents the vertical distance from outside the excavation to the rear wall of the box-type retaining wall;  $H$  denotes the depth from the ground surface, and  $H_e$  indicates the excavation depth of the foundation pit. As observed in the figure, the ground surface settlement outside the excavation exhibits a “spoon-shaped” profile.

The contour plots of settlement and rebound displacement after each excavation stage, as depicted in Figure 8, reveal that each excavation results in soil rebound at the pit bottom and settlement of the soil surrounding the foundation pit. Given the presence of buildings surrounding the foundation pit, to investigate the impact of unsupported excavation on the settlement of adjacent soil, a simulation was conducted using software to calculate the settlement values of the surrounding surface soil after each excavation stage. The results were plotted as a curve, as shown in Figure 9, exhibiting an overall “spoon-shaped” pattern, which aligns with the typical settlement patterns observed in foundation pit excavation. Following the completion of the third excavation stage, the maximum settlement of 4.25 mm was recorded in the surrounding soil at a distance of 31.85 m from the pit edge, which falls below the warning threshold of 20 mm set for this project. Moreover, the initial settlement values under different layer excavations will have different values. The reason for the varying starting points is that, after each excavation is completed, there is a need to wait for the release of soil stress and soil expansion. The soil at the edge of the box-type retaining wall is affected by the excavation of the foundation pit and will undergo expansion. However, as the distance from the edge of the foundation pit increases, soil settlement gradually enlarges, reaching a maximum value before slowly decreasing thereafter.

**FLAC3D 7.00**  
©2020 Itasca Consulting Group, Inc.

Zone Z Displacement



(a)

Figure 7. Cont.

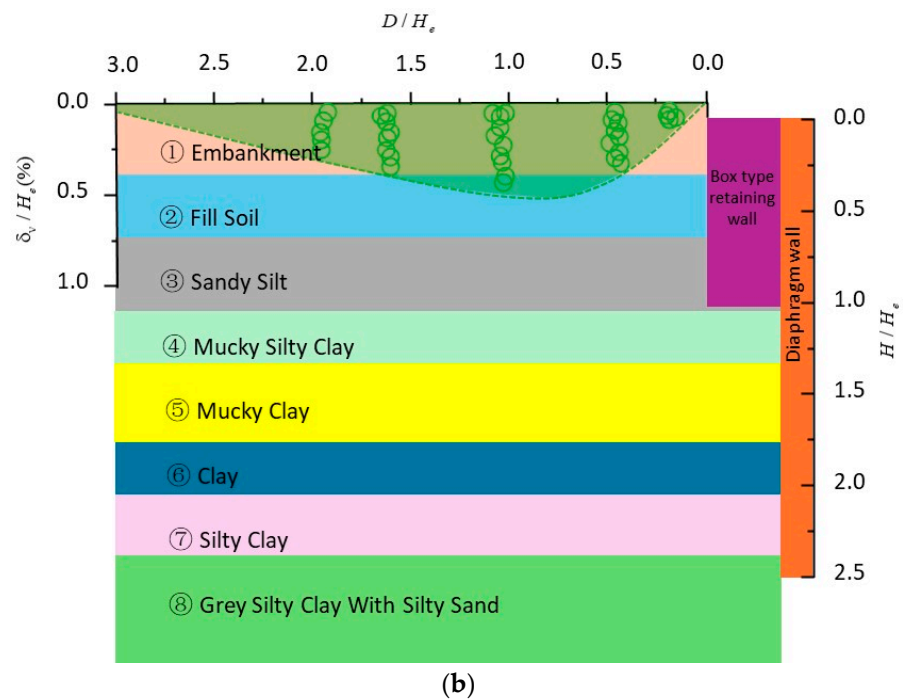


Figure 7. (a) Settlement curve of the foundation pit. (b) The influence zone behind the wall.

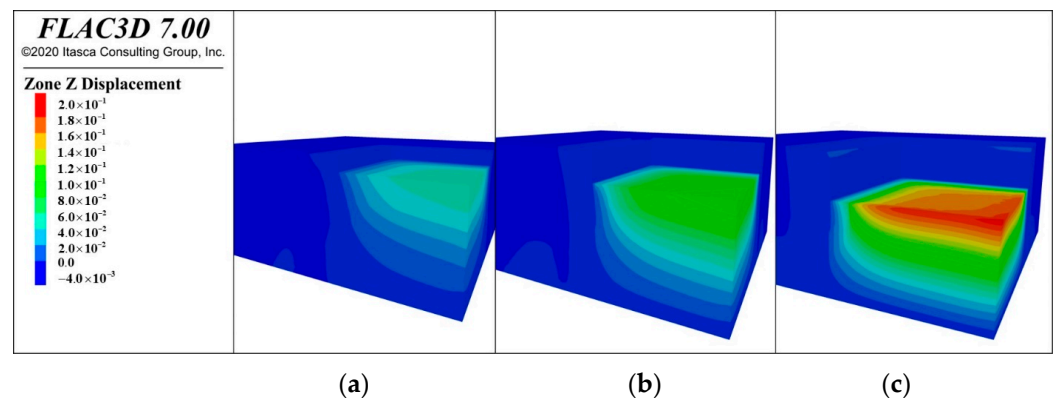


Figure 8. Settlement cloud map after excavation at different steps: (a) first layer excavation; (b) second layer excavation; (c) third layer excavation.

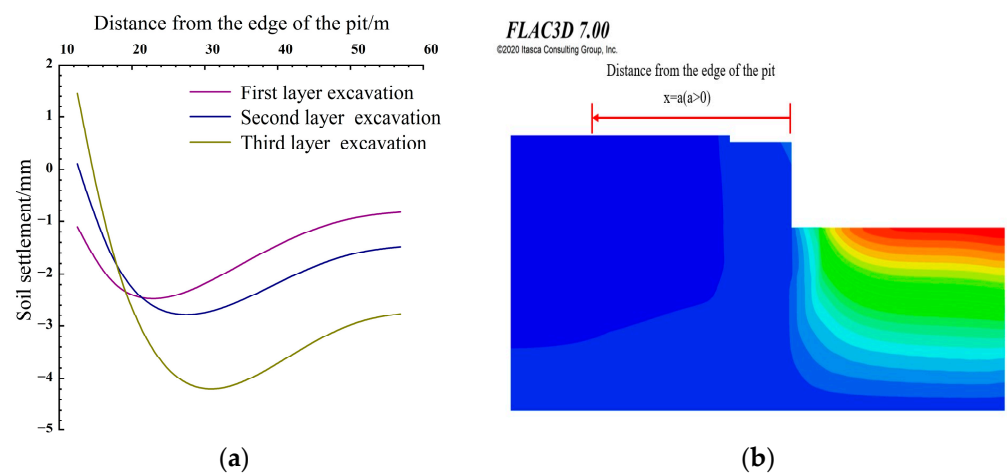
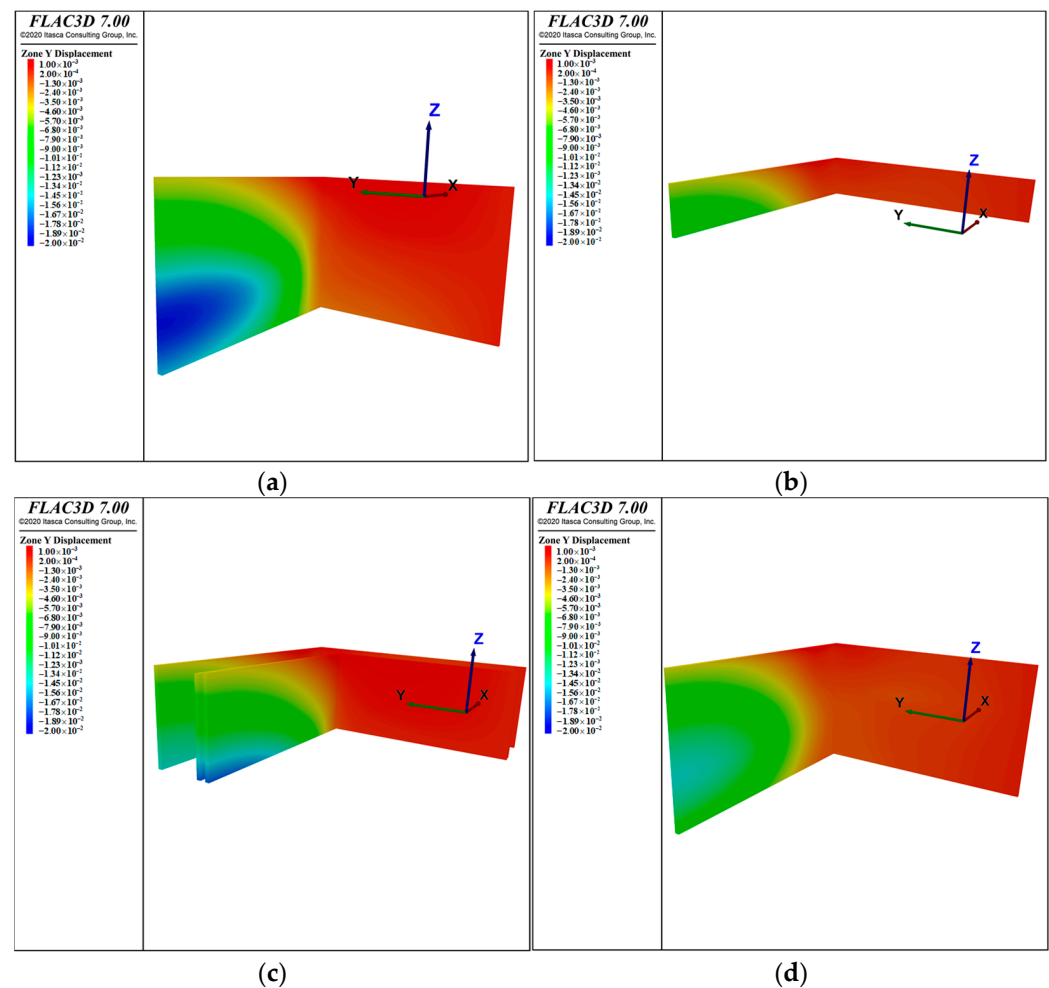


Figure 9. (a) Numerical simulation of soil settlement curve around foundation pit; (b) schematic diagram of the distance from the edge of the pit.

#### 4.2. Horizontal Displacement of Support Structure

Assuming the simulation results are reasonable, the analysis is conducted after the completion of excavation under this working condition. Using FLAC-3D software, horizontal displacement contour maps of the underground diaphragm wall, the rear wall of the box-type retaining wall, tri-axial soil mixing piles, and bored piles are obtained through computational simulations.

Based on the analysis of Figure 10, the maximum horizontal displacement of the underground diaphragm wall occurs at a depth of 25 m, with a value of  $-19.37$  mm. The overall displacement of the wall within the soft soil layer in the mid-to-lower sections is larger compared to the upper sections. The rear wall of the box-type retaining wall exhibits a maximum horizontal displacement of  $-11.72$  mm at a depth of 13.6 m from the bottom. The tri-axial soil mixing piles show a maximum horizontal displacement of  $-17.76$  mm at the bottom, at a depth of 33 m. The bored piles have a maximum horizontal displacement of  $-14.28$  mm at a depth of 20 m. According to the “Technical Standard for Monitoring of Construction Foundation Pit Engineering” [30], the threshold for retaining structures in this project is set at 20 mm. The simulation results from the software are all below the monitoring alert value. The maximum displacement locations of various supporting structures in the three-dimensional contour maps are primarily located near the soft soil layers, which is consistent with the deformation patterns of foundation pits, indirectly validating the reliability of the numerical simulation results.



**Figure 10.** Displacement cloud diagram of each supporting structure: (a) Underground diaphragm wall; (b) Back wall of box-type retaining wall; (c) Three-axis mixing pile; (d) Bored pile.

#### 4.3. Discussion of Influencing Factors on the Supporting Structure

During the support process of deep-foundation pits, due to the necessity of excavating the soil inside the pit after the construction of the box-type retaining wall, the “two-wall-in-one” construction method is adopted, which integrates the underground diaphragm wall with the inner lining wall. This design represents an optimized application of underground diaphragm walls in deep-foundation pit engineering. In this project, a novel box-type retaining wall is constructed in conjunction with the underground diaphragm wall. To investigate the factors influencing the horizontal displacement of this supporting structure, numerical simulation methods are utilized to analyze the displacement of the supporting structure from three aspects, thereby identifying the key influencing factors.

##### (1) Analysis of the influence of box-type retaining wall dimensions

When analyzing the impact of the box-type retaining wall dimensions on the “two-wall-in-one” support structure and the surface settlement behind the wall, both the length and width were varied within the original dimension range of 3 m. Specifically, when altering the length, the width was kept constant, and vice versa for changes in width. To investigate the effect of length variation on the deformation of the foundation pit retaining structure, the length of the box-type retaining wall was varied while maintaining its width and material properties constant. Seven lengths of 13, 12, 11, 10, 9, 8, and 7 m were considered. The displacement of the front wall under different lengths was analyzed. Negative values indicate displacement toward the inside of the foundation pit, and positive values indicate displacement in the opposite direction. Using finite element software to calculate the displacement of the wall under different lengths, a graphical analysis was conducted. As shown in Figure 11a, the displacement patterns of the wall are essentially the same, exhibiting a “spindle-shaped” distribution, which aligns with the typical displacement variation patterns observed in retaining structures during foundation pit excavation. As the length increases, the displacement of the front wall initially increases linearly. Due to the soft soil layer, the displacement amplification becomes more pronounced at −15 m, and the maximum displacement is reached at −25 m. As the foundation pit depth continues to increase, the retaining wall displacement gradually decreases. At a length of 13 m for the box-type retaining wall, the maximum displacement is 20.03 mm. As the length of the box-type retaining wall is gradually reduced, the maximum horizontal displacement of the wall also decreases, with approximately a 7% reduction in wall displacement for each 1 m decrease in length from 13 m. At a length of 7 m, the maximum displacement is 11.02 mm. The monotonic increase in wall displacement within the range of 7–13 m indicates that shorter intervals between box-type retaining walls result in greater overall stiffness, which better restricts the displacement of the foundation pit. As illustrated in Figure 11c, the box-type retaining wall has a width of 10.8 m. Surface settlement behind the wall is recorded starting from the 10.8 m mark along the length dimension. As the distance from the edge of the excavation pit increases, the settlement value reaches a maximum near 30 m and then gradually decreases thereafter. When the length of the box-type retaining wall is 7 m, the maximum settlement value is −2.4 mm. Conversely, when the length of the box-type retaining wall is 13 m, the maximum settlement value increases to −6.3 mm. These results indicate that shorter spacing between box-type retaining walls can enhance overall stiffness, thereby more effectively limiting surface settlement around the excavation pit.

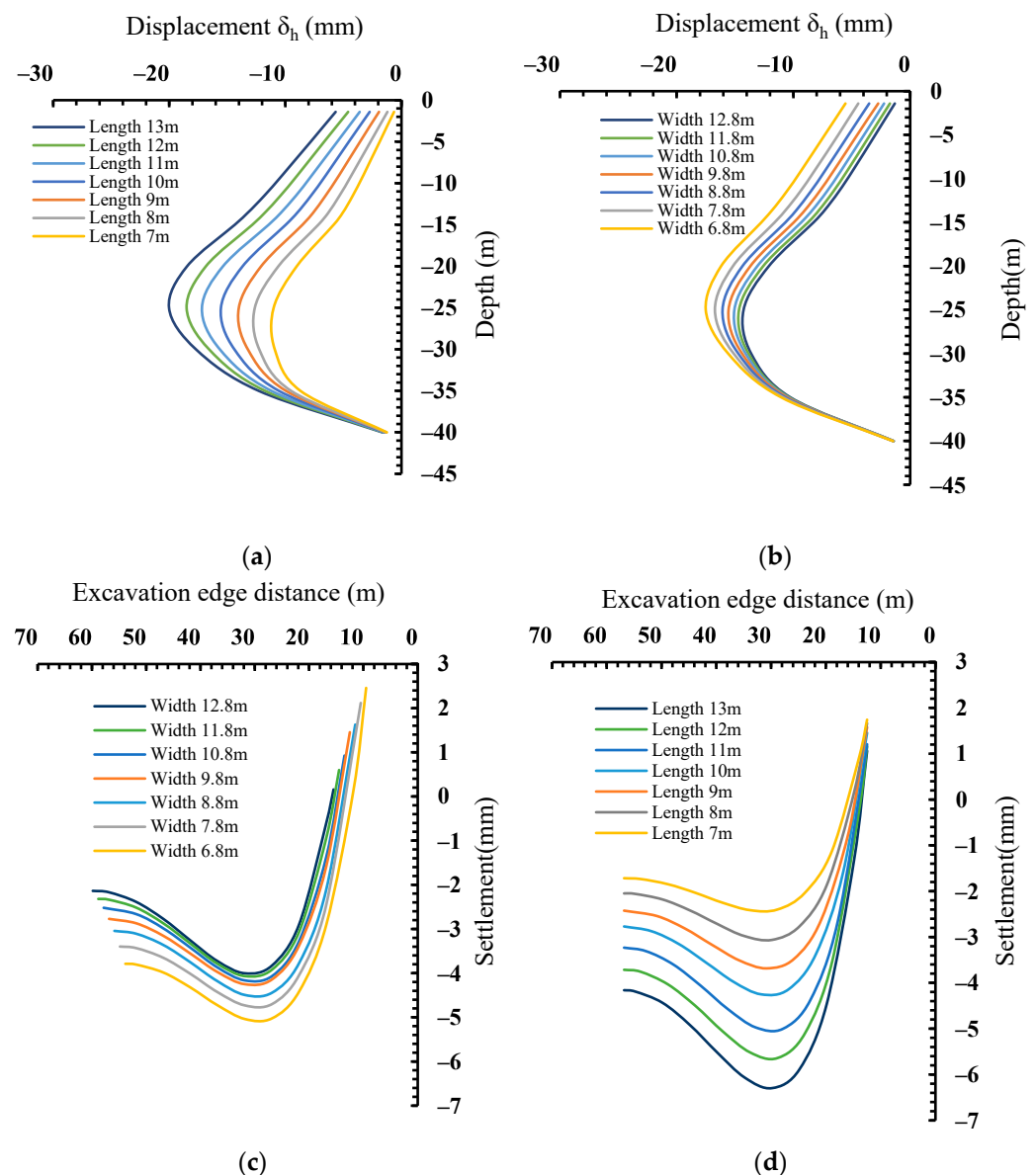


**Figure 11.** Influence of box-type retaining wall dimensions: (a,b) Horizontal displacements of front wall of box-type retaining wall; (c,d) Surrounding surface settlements with variations in the box length and width.

To investigate the effect of width variation on the deformation of the foundation pit retaining structure as well as the surface settlement behind the wall, the width of the box-type retaining wall was altered while keeping its length and material properties constant. Seven different widths of 12.8 m, 11.8 m, 10.8 m, 9.8 m, 8.8 m, 7.8 m, and 6.8 m were considered for the box-type retaining wall. The displacement of the front wall under these different widths was analyzed. As depicted in Figure 11b, when the length and material properties remain unchanged, the displacement patterns of the wall under varying widths are essentially the same, exhibiting similar trends to those observed with length variations. At a width of 6.8 m for the box-type retaining wall, the maximum displacement of the wall at a depth of 25 m reaches 17.51 mm, which is smaller compared to when varying the length. As the width increases from 6.8 m, the horizontal displacement of the wall gradually decreases. A reduction of approximately 2.5% to 6% in the maximum displacement is observed for every 1 m decrease in width. Wider retaining walls provide better restraint against wall displacement. As shown in Figure 11d, when the length and material properties of the box-type retaining wall remain constant, and with variations in

width, the surface settlement behind the wall generally reaches its maximum value near a distance of 30 m from the wall and then gradually decreases as the distance increases. When the width of the box-type retaining wall is 12.8 m, the maximum settlement value is 4.0 mm. For comparison, when considering a hypothetical scenario where the box length is 6.8 m, the maximum settlement value is 5.0 mm. Overall, the results indicate that variations in the width of the box-type retaining wall have a relatively minor impact on the settlement of the soil behind the wall;

## (2) Analysis of the influence of varying filler types within the retaining wall

When studying the influence of the internal fill material of box-type retaining walls on the “two-wall-in-one” support structure and the surface settlement behind the wall, the impact of different types of fill materials on foundation pit deformation was analyzed. Numerical calculations were performed for four scenarios (Table 3): using surface fill soil (Filler 1); hydraulic fill (Filler 2); mucky silty clay (Filler 3); and the absence of fill material (No filler). No filler means that the interior space of the box-type retaining wall remains empty without any filler.

**Table 3.** Table of physical and mechanical properties of fillers in retaining walls.

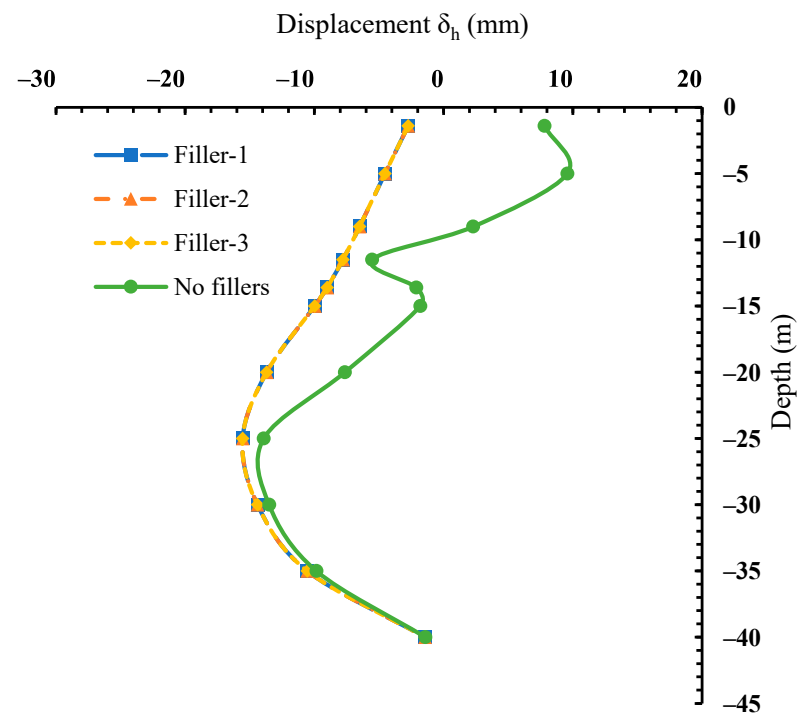
Filler Type	$\gamma$ kN/m <sup>3</sup>	$K_0$	$\nu$	$E$ /kPa	$c$ /kPa	$\varphi$ /(°)
Filler-1	17.8	0.380	0.281	27,180	15	27
Filler-2	18	0.350	0.259	31,140	12	15
Filler-3	17.7	0.510	0.338	19,140	10	16.8
No fillers	/	/	/	/	/	/

As illustrated in Figure 12a,b, under the same degree of compaction, whether high-quality soil or inferior silty clay is used as the fill material for the box-type retaining wall, the displacement variations in the wall and the soil behind it remain essentially consistent. This indicates that, according to the numerical simulation results, soil quality has a minor impact on the retaining effectiveness of the box-type retaining wall. When there is no fill material within the box, the retaining wall’s displacement above the foundation pit base becomes highly irregular, exhibiting abrupt changes in displacement and structural instability. The soil behind the wall experiences expansion, with settlement values continuously increasing, and the maximum settlement increases by 3 mm compared to cases with fill materials. Therefore, the inclusion of fill material within the box-type retaining wall is a necessary measure to achieve satisfactory retaining performance.

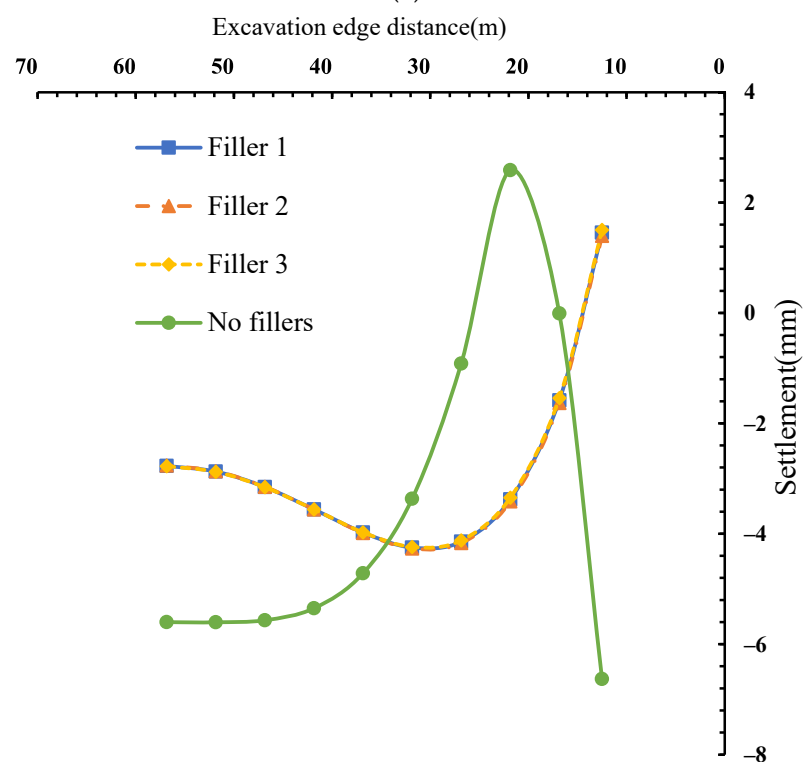
## (3) Analysis of the influence of cement materials in the box-type retaining wall

In investigating the impact of concrete materials used for pouring box-type retaining walls on the deformation of foundation pit retaining structures as well as the surface settlement behind the wall, the variations in the displacement of the box-type retaining walls cast with C20, C30, C40, and C50 concrete were compared. The parameters of the concrete materials are presented in Table 3. As shown in Figure 13, it can be observed that the displacements of the front and back walls of the retaining wall, as well as the surface settlement behind the wall, are essentially the same. By using concrete of varying materials to pour the box-type retaining walls, it is evident that stronger concrete exhibits better performance in restricting wall displacement compared to weaker concrete. However, the influence on the horizontal displacement of the retaining wall and the surface settlement behind the wall is not significant. The results presented in Figure 13 indicate that the displacement of the front wall of the retaining wall remains essentially consistent. When constructing box-type retaining walls using concrete of different materials, increasing the

concrete strength is more effective in limiting wall displacement than using lower-strength concrete. However, the impact on the horizontal displacement of the retaining wall and the settlement of the soil behind the wall remains relatively minor.

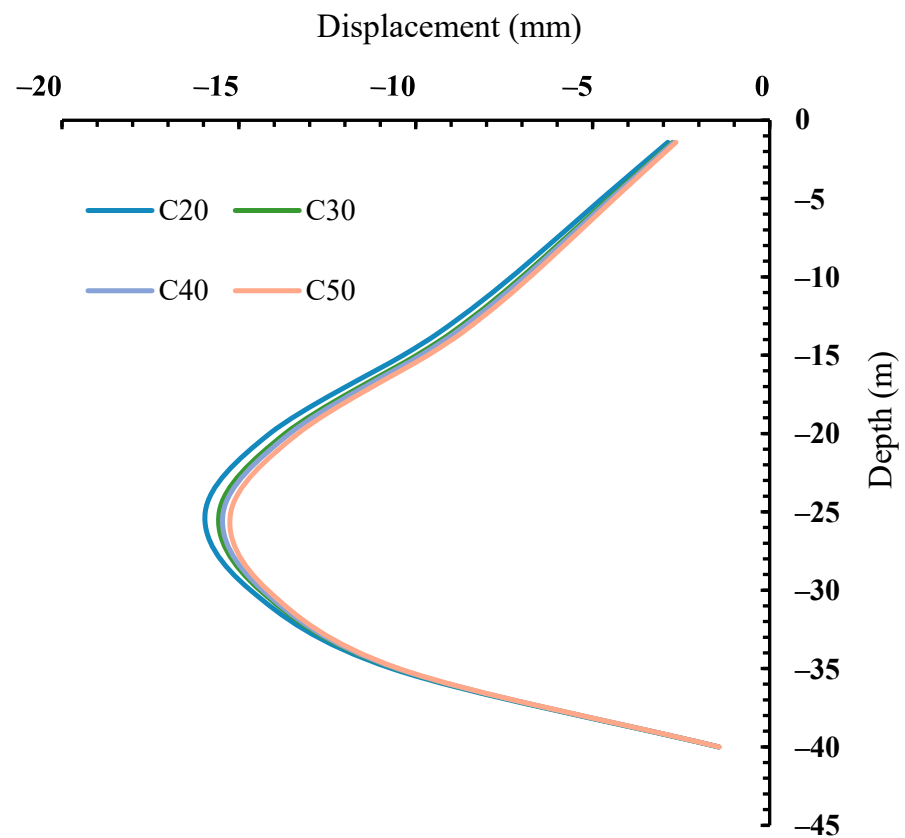


(a)

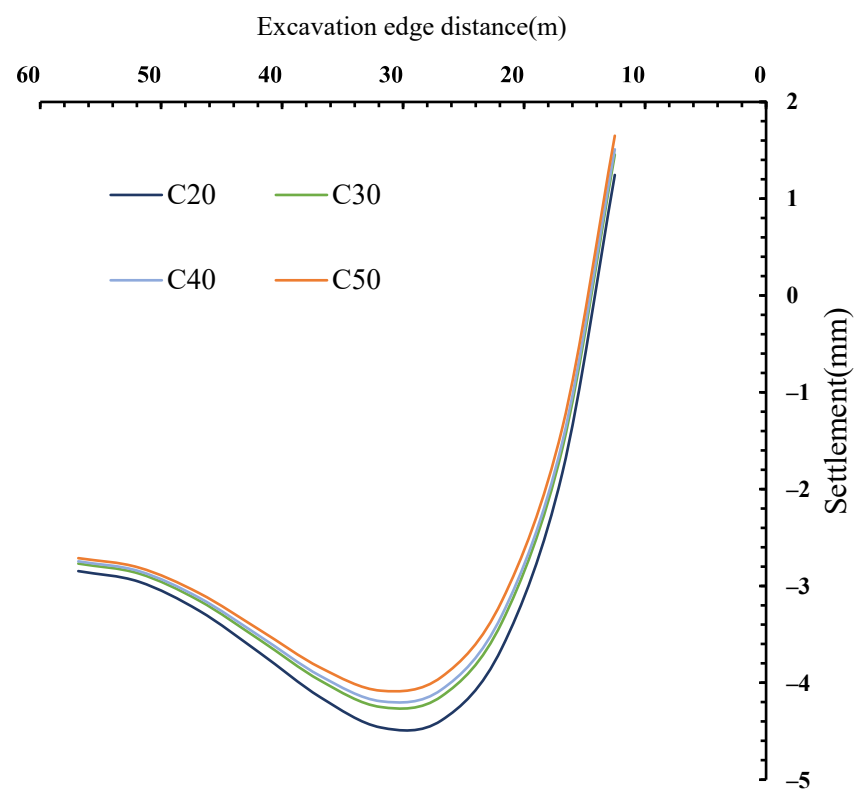


(b)

**Figure 12.** Influence of the internal fill material of box-type retaining walls: (a) Horizontal displacement of the front wall of box-type retaining wall; (b) settlement of the surrounding surface from the edge of foundation pit.



(a)



(b)

**Figure 13.** Influence of concrete materials used for pouring box-type retaining walls: (a) Horizontal displacement of the front wall of box-type retaining wall; (b) settlement of the surrounding surface from the edge of foundation pit.

## 5. Conclusions

Based on the foundation pit construction of a wastewater treatment plant in Shanghai, a three-dimensional numerical model of the pit and retaining wall structure was established using the FLAC 3D simulation method. The lateral deformation of the support structure at different construction stages of the deep-foundation pit, as well as the surrounding surface settlement responses, were studied. The main conclusions are as follows:

- (1) In soft soil foundation deep excavation projects, the novel box-type retaining wall demonstrates remarkable support performance. Compared to other types of retaining walls, it boasts advantages such as simple structure, unsupported excavation construction, and convenient sourcing of filling materials. Key factors influencing the support effectiveness of the box-type retaining wall were analyzed, focusing on three aspects: wall dimensions; filling materials within the box; and constituent materials;
- (2) During foundation pit excavation, rebound appears at the center, while settlement occurs at the edges. Simulations analyzed the impact of box-type retaining wall dimensions, fill materials, and constituent materials on settlement. Results showed that dimension changes caused settlement variations of 1–3 mm. Except for the no-fill condition causing soil expansion and continuous settlement, settlement trends were consistent under the other three fill conditions. Changes in constituent materials had insignificant effects on settlement;
- (3) By altering the dimensions of the box-type retaining wall, it was observed that when the wall width was held constant, a reduction of 1 m in wall length led to approximately a 7% decrease in wall displacement at the base of the excavation pit. Conversely, when the wall length was held constant, a reduction of 1 m in wall width resulted in approximately a 6.8% increase in wall displacement at the base;
- (4) The advantages of adopting box-type retaining walls are as follows: (a) enabling unsupported excavation construction; (b) featuring a simple structure, primarily filled with plain soil and stone materials; (c) demonstrating excellent stability, high shear strength, and adaptability to various foundation types; (d) resulting in significant savings in concrete materials; (e) serving as a permanent exterior wall structure when integrated with retaining piles, thereby enhancing the overall rigidity, stability, safety, and reliability of the retaining system.

This paper mainly adopts the method of numerical simulation to study the performance of box-type retaining walls in controlling deformation. Further research can combine long-term observations and data analysis to investigate and discuss the long-term usability of this novel structure. Additionally, since this research involves water-treatment facilities, potential environmental threats (such as permeability, corrosion of concrete structures, and strength loss after corrosion) can be further discussed in the future.

**Author Contributions:** Conceptualization, P.P. and W.K.; methodology, W.K. and Y.L. (Yi Long); software, S.H. and Y.L. (Yi Long); validation, P.P., W.K. and Y.L. (Yang Lu); writing—original draft preparation, W.K., Y.L. (Yi Long) and Y.L. (Yang Lu); writing—review and editing, P.P., W.K., Y.L. (Yi Long) and Y.L. (Yang Lu). All authors have read and agreed to the published version of the manuscript.

**Funding:** This research received no external funding.

**Data Availability Statement:** The data are contained within this article.

**Acknowledgments:** The authors wish to express their gratitude to the anonymous reviewers whose constructive comments helped to improve the overall quality of this paper.

**Conflicts of Interest:** Authors Peng Peng, Weiyao Kong, Saishuai Huang were employed by the company Shanghai Municipal Engineering Design Institute (Group) Co., Ltd. The remaining authors declare that the research was conducted in the absence of any commercial or financial relationships that could be construed as a potential conflict of interest.

## References

1. Giwa, A.S.; Ali, N. An extensive analysis of the engineering design of underground sewage plants in China. *Processes* **2023**, *11*, 3010. [\[CrossRef\]](#)
2. Lan, B.; Wang, Y.; Wang, W. Review of the double-row pile supporting structure and its force and deformation characteristics. *Appl. Sci.* **2023**, *13*, 7715. [\[CrossRef\]](#)
3. Xu, Q.; Xie, J.; Sun, Z.; Lu, L.; Yu, H. Stability Analysis of Trench Wall for Diaphragm Wall in Ultra-Deep Circular Foundation Pit: A Comprehensive Investigation. *Appl. Sci.* **2023**, *13*, 12037. [\[CrossRef\]](#)
4. Peng, H.; Meng, B.; Tan, S.; Zhu, L.; Wang, G. Study on Deformation Control of Road-Deep Foundation Pit Passing under Elevated Subway Bridge. *Appl. Sci.* **2024**, *14*, 6357. [\[CrossRef\]](#)
5. Wang, J.; Deng, Y.; Wang, X.; Liu, X.; Zhou, N. Numerical evaluation of a 70-m deep hydropower station foundation pit dewatering. *Environ. Earth Sci.* **2022**, *81*, 364. [\[CrossRef\]](#)
6. Salgado, R. *The Engineering of Foundations, Slopes and Retaining Structures*; CRC Press: Boca Raton, FL, USA, 2022; ISBN 9781315213361.
7. Dhamdhere, D.R.; Rath, V.R.; Kolase, P.K. Design and analysis of retaining wall. *Int. J. Manag. Technol. Eng.* **2018**, *8*, 1246–1263.
8. Wang, S.; Xu, L.; Zhang, X.; Long, L.; Zhuang, X. Development and Field Analysis of a Novel Servo Concrete Bracing System for Deep Foundation Pit Excavation. *Buildings* **2024**, *14*, 1674. [\[CrossRef\]](#)
9. Niu, Y.; Zou, L.; Wang, Q.; Ma, F. Study on deformation characteristics of retaining structures under coupled effects of deep excavation and groundwater lowering in the affected area of fault zones. *Sustainability* **2023**, *15*, 8060. [\[CrossRef\]](#)
10. Gui, M.W.; Rajak, R.P. A Numerical Study of a Soil-Nail-Supported Excavation Pit Subjected to a Vertically Loaded Strip Footing at the Crest. *Buildings* **2024**, *14*, 927. [\[CrossRef\]](#)
11. Kong, W.Y. Analysis on the Selection of Retaining and Supporting Systems for Extra-Large Deep Foundation Pit Engineering in Soft Soil Areas. *Urban Roads Bridges Flood Control* **2018**, 141–144+17–18. [\[CrossRef\]](#)
12. Wang, J.C. Key technology for construction of box type retaining wall enclosure structure for a deep foundation pit in soft soil area. *China Munic. Eng.* **2020**, 84–86. [\[CrossRef\]](#)
13. Chikute, G.C.; Sonar, I.P. Gabion Wall: Eco-friendly and Cost-Efficient Retaining Wall. In *Advances in Sustainable Construction Materials: Select Proceedings of ASCM 2020*; Springer: Singapore, 2020; pp. 229–249.
14. Hirai, T.; Otani, J. Behavior of geogrid reinforced soil wall using box-type wall. *Geosynth. Eng. J.* **1998**, *13*, 355–363. [\[CrossRef\]](#)
15. Ramli, M.; Karasu, T.; Dawood, E.T. The stability of gabion walls for earth retaining structures. *Alex. Eng. J.* **2013**, *52*, 705–710. [\[CrossRef\]](#)
16. Wang, J.L. Study on the Distribution Law of Displacement and Soil Pressure of Retaining Walls and Stability Analysis of Box Type Retaining Walls. Master's Thesis, Northwest A&F University, Yangling, China, 2010.
17. Wang, S. Research on the Optimal Design of Box-Type Gravity Concrete Retaining Walls. Ph.D. Thesis, Chang'an University, Chang'an, China, 2012.
18. GBT50123; Ministry of Housing and Urban-Rural Development of the People's Republic of China. Standards for Geotechnical Test Methods: Beijing, China, 2019.
19. Augarde, C.E.; Lee, S.J.; Loukidis, D. Numerical modelling of large deformation problems in geotechnical engineering: A state-of-the-art review. *Soils Found.* **2021**, *61*, 1718–1735. [\[CrossRef\]](#)
20. Lou, C.H.; Xia, T.D.; Liu, N.W. Spatial effect analysis of the impact of foundation pits on the surrounding environment in soft soil areas. *Chin. J. Geotech. Eng.* **2019**, *41*, 249–252.
21. Li, D.; Yi, F.; Li, X.; Chen, S.; Hu, Z.; Liu, J. Excavation Effects on Reinforced Concrete Pile Foundations: A Numerical Analysis. *Buildings* **2024**, *14*, 995. [\[CrossRef\]](#)
22. Gao, X.; Tian, W.P.; Zhang, Z. Analysis of deformation characteristics of foundation-pit excavation and circular wall. *Sustainability* **2020**, *12*, 3164. [\[CrossRef\]](#)
23. Song, F.; Wang, H.; Shang, C.; Rodriguez-Dono, A.; Wang, E.; Gui, J.; Alejano, L. Considering creep in rock tunnelling with a combined support system: Theoretical solutions and machine-learning solver. *Tunn. Undergr. Space Technol.* **2024**, *153*, 106019. [\[CrossRef\]](#)
24. Mao, H.; Hu, Z.; Wang, W.; Liu, Z.; Yang, H.; Li, B.; Wang, Y. Two-Stage Analysis Method for the Mechanical Response of Adjacent Existing Tunnels Caused by Foundation Pit Excavation. *Buildings* **2024**, *14*, 2246. [\[CrossRef\]](#)
25. Song, F.; Gens, A.; Collico, S.; Plúa, C.; Armand, G.; Wang, H. Analysis of thermally-induced fracture of Callovo-Oxfordian claystone: From lab tests to field scale. *Geomech. Energy Environ.* **2024**, *39*, 100579. [\[CrossRef\]](#)

26. Chen, S.; Cui, J.; Liang, F. Case study on the deformation coupling effect of a deep foundation pit group in a coastal soft soil area. *Appl. Sci.* **2022**, *12*, 6205. [[CrossRef](#)]
27. Zhu, J.; Qian, F.; Cai, J. Research on a Calculation Method for the Horizontal Displacement of the Retaining Structure of Deep Foundation Pits. *Buildings* **2024**, *14*, 1694. [[CrossRef](#)]
28. Xian, Q.; Wang, Z.; Liu, X.; Ma, S.; Xiao, Z. Site Measurement Study on Mechanical Properties of SMW Piles of Building Structures in Sandy Soil Areas. *Buildings* **2022**, *12*, 1733. [[CrossRef](#)]
29. Jiang, Z.; Zhu, S.; Que, X.; Ge, X. Deformation Effects of Deep Foundation Pit Excavation on Retaining Structures and Adjacent Subway Stations. *Buildings* **2024**, *14*, 2521. [[CrossRef](#)]
30. GB50497; Ministry of Housing and Urban-Rural Development of the People's Republic of China. Technical Standard for Monitoring of Building Excavation Engineering: Beijing, China, 2019.

**Disclaimer/Publisher's Note:** The statements, opinions and data contained in all publications are solely those of the individual author(s) and contributor(s) and not of MDPI and/or the editor(s). MDPI and/or the editor(s) disclaim responsibility for any injury to people or property resulting from any ideas, methods, instructions or products referred to in the content.